

GaBoDS: The Garching-Bonn Deep Survey

II. Confirmation of EIS cluster candidates by weak gravitational lensing^{*}

M. Schirmer¹, T. Erben¹, P. Schneider¹, C. Wolf², and K. Meisenheimer³

¹ Institut für Astrophysik und Extraterrestrische Forschung (IAEF), Universität Bonn, Auf dem Hügel 71, 53121 Bonn, Germany

² Department of Physics, Denys Wilkinson Bldg., University of Oxford, Keble Road, Oxford, UK

³ Max-Planck-Institut für Astronomie, Königstuhl 17, 69117 Heidelberg, Germany

Received 21 January 2004 / Accepted 8 March 2004

Abstract. We report the first confirmation of colour-selected galaxy cluster candidates by means of weak gravitational lensing. Significant lensing signals were identified in the course of the shear-selection programme of dark matter haloes in the Garching-Bonn Deep Survey, which currently covers 20 square degrees of deep, high-quality imaging data on the southern sky. The detection was made in a field that was previously covered by the ESO Imaging Survey (EIS) in 1997. A highly significant shear-selected mass-concentration perfectly coincides with the richest EIS cluster candidate at $z \approx 0.2$, thus confirming its cluster nature. Several other shear patterns in the field can also be identified with cluster candidates, one of which could possibly be part of a filament at $z \approx 0.45$.

Key words. cosmology: dark matter – galaxies: clusters: general – cosmology: gravitational lensing

1. Introduction

The search for dark matter haloes by weak gravitational lensing was first proposed by Kaiser (1995) and Schneider (1996) (hereafter S96). Using this technique, clusters are detected directly by their mass instead of their luminosity, and no assumptions have to be made about their virial state or the relation between bright and dark matter. In this way, a mass-selected cluster sample can be established, and the cluster population can be probed e.g. for underluminous objects. With moderately sized telescopes, however, this method is restricted to haloes in the intermediate redshift range (up to $z \approx 0.6$), since with an increasing lens distance the population of sheared background galaxies is shifted to higher redshifts, making their shape measurement increasingly difficult.

Kruse & Schneider (1999) predicted the number density of shear-selectable galaxy clusters with $S/N \geq 5$ to be of the order of 10 deg^{-2} . This figure is based on optimistic estimates of the width of the ellipticity distribution of galaxies and their accessible number density. With 2 m-class telescopes, the number of such clusters per deg^{-2} is about a factor of 5–10 smaller. Since the advent of wide field imagers, a number of

shear-selected dark matter haloes were reported in the literature (see Erben et al. 2000; Umetsu & Futamase 2000; Maoli et al. 2001; Wittman et al. 2001, 2002; Miralles et al. 2002; Miyazaki et al. 2002; Dahle et al. 2003; Schirmer et al. 2003, for example). About half of these objects have optical counterparts, the nature of the others remains unclear.

In this work we present a sample of shear-selected dark matter haloes which (mostly) coincide with colour-selected galaxy cluster *candidates*. The objects were found in one of the 63 fields of the Garching-Bonn Deep Survey (hereafter GaBoDS), which are currently analysed in this respect. Section 2 summarises the observations and the data reduction, and Sect. 3 presents the *mass aperture statistics* (see S96) used for the shear selection. The particular detections are presented in Sect. 4, and we draw conclusions in Sect. 5.

2. Observations and data reduction

GaBoDS is a mostly virtual survey, with 80% of the data taken from the ESO archive or contributed by collaborators. It covers a sky area of currently 20 square degrees taken with the Wide Field Imager (WFI) at the MPG/ESO 2.2 m telescope. The outstanding image quality of this instrument makes it ideally suited for observations of the weak lensing effect.

Send offprint requests to: M. Schirmer,
e-mail: mischa@astro.uni-bonn.de

* Based on observations made with ESO Telescopes at the La Silla Observatory.

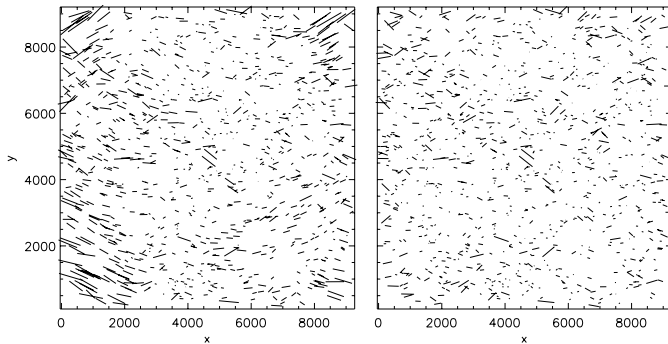


Fig. 1. PSF anisotropies in the stacked SGP image. The pattern is mostly due to slight misalignments of the CCDs with respect to the focal plane. *Left:* before correction, *right:* after correction. Coherent distortion patterns are largely removed from the data. The largest stick lengths in the left panel correspond to anisotropies of 1.5%.

The field (“SGP”) under consideration is centred on the South Galactic Pole and was observed during MPG time in the course of the COMBO-17 project (see Wolf et al. 2003). Observations in R -band were carried out in October 1999 and September 2000. The total exposure time amounts to 27 ks (7.5 h) dark time, 20 ks of which were selected for the coaddition due to their sub-arcsecond seeing quality and PSF properties.

The data reduction was performed with the GaBoDS pipeline, which was specifically developed for the reduction of any kind of WFI data. A detailed description of the algorithms involved and their performance can be found in Schirmer et al. (2003). Specific care was taken for the relative astrometric calibration of the individual CCDs. The accuracy obtained is on the order of a 1/10th–1/20th of a pixel, thus no artificial anisotropies are introduced into the PSF (Fig. 1) that could mimic a shear signal. The seeing in the coadded image ($35' \times 37'$) is $0''.8$, and we reach a limiting magnitude of $R = 26.1$ (Vega) for objects with at least 4 connected pixels 2.5σ above the sky background. The measurement of the galaxy shapes and the correction for PSF effects was performed with the KSB software (Kaiser et al. 1995). A detailed description and test of our implemented shape measurement approach is given in Erben et al. (2001).

3. The shear-selection method

In the following, standard weak lensing notations are used. For a technical review of this topic see Bartelmann & Schneider (2001).

The tidal gravitational field of a cluster-sized mass concentration induces a coherent distortion pattern in the images of distant background galaxies. By scanning the field for such characteristic patterns, the causing mass concentrations can be found. For the detection of these shear patterns we use the *mass aperture statistics* (M_{ap} , see S96). There, M_{ap} is defined as a filtered integral of the projected lens mass distribution κ inside an aperture. Switching to a different filter function, κ can be replaced by the tangential shear γ_t , for which the observable

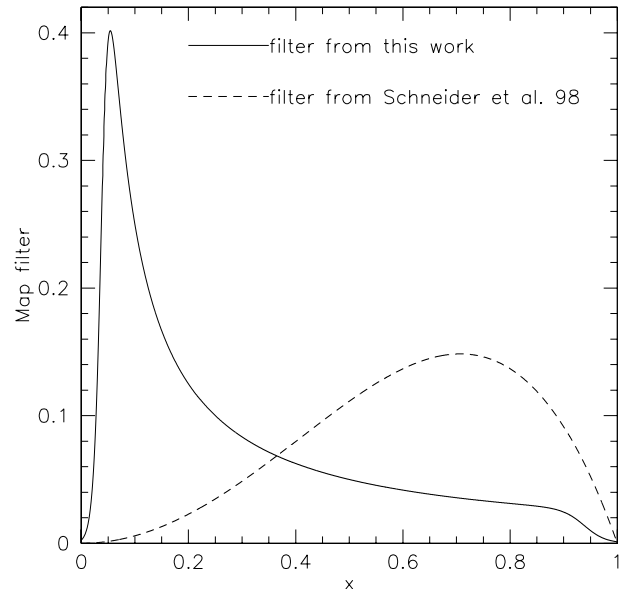


Fig. 2. The plot compares the M_{ap} filter from this work with that proposed in Schneider et al. (1998). The x -axis shows the distance from the aperture centre in units of the aperture size.

ellipticities ϵ_t of the background galaxies are an unbiased estimator. On a discrete grid M_{ap} evaluates as

$$M_{\text{ap}} = \frac{\sum_i \epsilon_{ti} w_i Q_i}{\sum_i w_i}, \quad (1)$$

where ϵ_{ti} are the tangential components of the ellipticities of the lensed galaxies. The w_i are individual weighting factors as introduced by Erben et al. (2001), and Q_i is the M_{ap} filter function. The noise for M_{ap} is obtained as

$$\sigma^2(M_{\text{ap}}) = \frac{\sum_i |\epsilon_{ti}|^2 w_i^2 Q_i^2}{2 (\sum_i w_i)^2}, \quad (2)$$

so that the ratio $S = M_{\text{ap}}/\sigma(M_{\text{ap}})$ directly estimates the signal-to-noise of the shear-selected dark matter halo detection. We call this quantity the *S-statistics*, and its two-dimensional graphical representation the *S-map*. We assume a flat cosmology with $\Omega_0 = 0.3$, $\Omega_\Lambda = 0.7$ and a Hubble parameter of $h = 0.7$.

We use a different filter function Q than the ones proposed in S96 and in Schneider et al. (1998), approximating the expected tangential shear profile of a NFW halo with a singular isothermal sphere (see Fig. 2). The filter is cut-off for very small and very large radii. The differences between a NFW- and a SIS-filter in terms of cluster detection are marginal only, but the latter has computational advantages.

Note that M_{ap} is not any more directly related to the mass inside the aperture once it is evaluated near the border of the

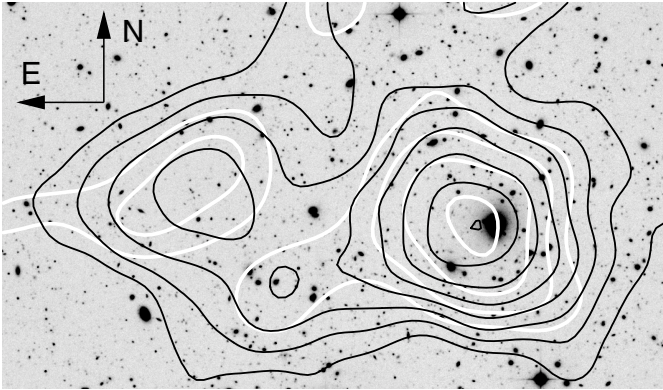


Fig. 3. Shear-selection of EIS0045–2923, detected at the 5.5σ -level. The black contours show the significance of the tangential shear found around the position under consideration, starting at 2σ and increasing in steps of 0.5σ . The white contours show the reconstructed surface mass density, starting with $\kappa = 0.05$ and increasing in steps of 0.03 for a smoothing length of $2''.0$. The agreement between the two contour types is very good. The field shown is $7'.3 \times 4'.3$ wide.

field, or on a galaxy distribution with swiss-cheese topology (e.g. due to masking of bright stars). However, the S -statistics itself is unaffected by this and can be used to detect dark matter haloes, since M_{ap} still estimates the amount of shear alignment inside the aperture. More details of this and a thorough discussion of filter functions will be found in Schirmer et al. (2004, in preparation), in which a shear-selected sample of about 100 mass concentrations based on the 20 square degrees of GaBoDS will be presented.

4. Results

Our weak shear detections in the SGP field are presented in Fig. 4. Shown are the contours of the S -map for a filter scale of $20''$. The number density of galaxies was $n = 24 \text{ arcmin}^{-2}$. The optical counterparts were selected in V and I by Olsen et al. (1999, hereafter EIS) and Lobo et al. (2000, hereafter LIL), both using the EIS Wide Survey Patch B field and the matched filter algorithm by Postman et al. (1996). The authors estimate the redshifts of these candidates based on the colour of their elliptical galaxies.

Most prominently, EIS0045–2923 ($z \approx 0.2$) is detected at the 5.5σ -level (Fig. 3). A mass reconstruction according to the finite field algorithm of Seitz & Schneider (1996) is shown, too. The mass sheet degeneracy is broken by the assumption that on average κ vanishes on the image border. Based on the reconstruction we derive a cluster mass of $(6 \pm 2) \times 10^{14} M_{\odot}$ within a radius of 260 kpc at the cluster redshift, assuming that the lensed galaxies are at $z = 1$. EIS0045–2923 is the richest cluster candidate as identified by EIS, even though it looks rather poor in the R -band image (as do all the other candidates), with a single cD galaxy. A significant extension to the east is visible, in the middle of which about half a dozen ellipticals at possibly higher redshift are found.

$11'$ east of EIS0045–2923, a 3.6σ -detection coincides with LIL004608–292341 ($z \approx 0.45$). The galaxies therein form two strongly interacting subgroups. $1.5'$ further to the South is EIS0046–2925 ($z \approx 0.2$), which is not seen in any of our S -maps. The lensing contours extend towards the East on a significant level for filter scales from 7–20 arcmin. $6'.5$ (2.2 Mpc) into this direction we have LIL004636–293539 ($z \approx 0.4$ –0.5), falling slightly outside the S -contours. If these two clusters are indeed at the same redshift, this could indicate the presence of a filament. For another weak lensing detected filament see for example Gray et al. (2002).

When looking at the S -map for the full SGP field, the detections for EIS0045–2923 and LIL004608–292341 stand out remarkably clear over the rest of the field, as well as in their size as in their significance. In Fig. 4 several other EIS and LIL cluster candidates are indicated. The 2σ -detection next to EIS0045–2948 in Fig. 4 rises up to 4.3σ for a smaller filter scale of $6'.3$, but is offset by $1'$ to the West. This is consistent with the rms offset we find for other mass concentration/optical counterpart pairs in our survey.

In order to rule out any remaining systematic effects inherent to the data, we split the 68 raw WFI images into two halves. One half contained only images with excellent PSF properties (better than 3% anisotropy), whereas the second one consisted of those with anisotropies up to 6% (mostly due to a slight defocusing of the telescope). The PSFs in the final stacks of the two sets look similar to the one shown in Fig. 1, since the individual anisotropies in defocused exposures rotate by 90 degrees when the detector plane passes through the focal plane, thus they average out in the coaddition. From these two entirely independent data sets we confirm the shear detections of EIS0045–2923 and LIL004608–292341, but with a lower S/N due to the reduced number density ($n = 19 \text{ arcmin}^{-2}$) of galaxies. The fluctuations of less significant peaks (<3 – 3.5σ) between the various realisations increase, especially when moving to filter scales below $10''$.

5. Conclusions

We presented a sample of shear-selected mass concentrations in a deep observation of the South Galactic Pole, which was previously covered by the EIS Wide Survey Patch B field. Two of the mass concentrations found coincide with the colour-selected cluster candidates EIS0045–2923 and LIL004608–292341, taken from the Patch B observations, and thus confirm their cluster nature. There is evidence for a possible filament connecting LIL004608–292341 with LIL004636–293539. A smaller mass concentration found is probably associated with EIS0045–2948. For the remaining low- S/N detections no conclusions could be reached. We have shown that the shear-selection method yields very useful results also for less massive clusters.

Acknowledgements. This work was supported by the BMBF through the DLR under the project 50 OR 0106, by the BMBF through DESY under the project 05AE2PDA/8, and by the Deutsche Forschungsgemeinschaft (DFG) under the project SCHN 342/3–1.

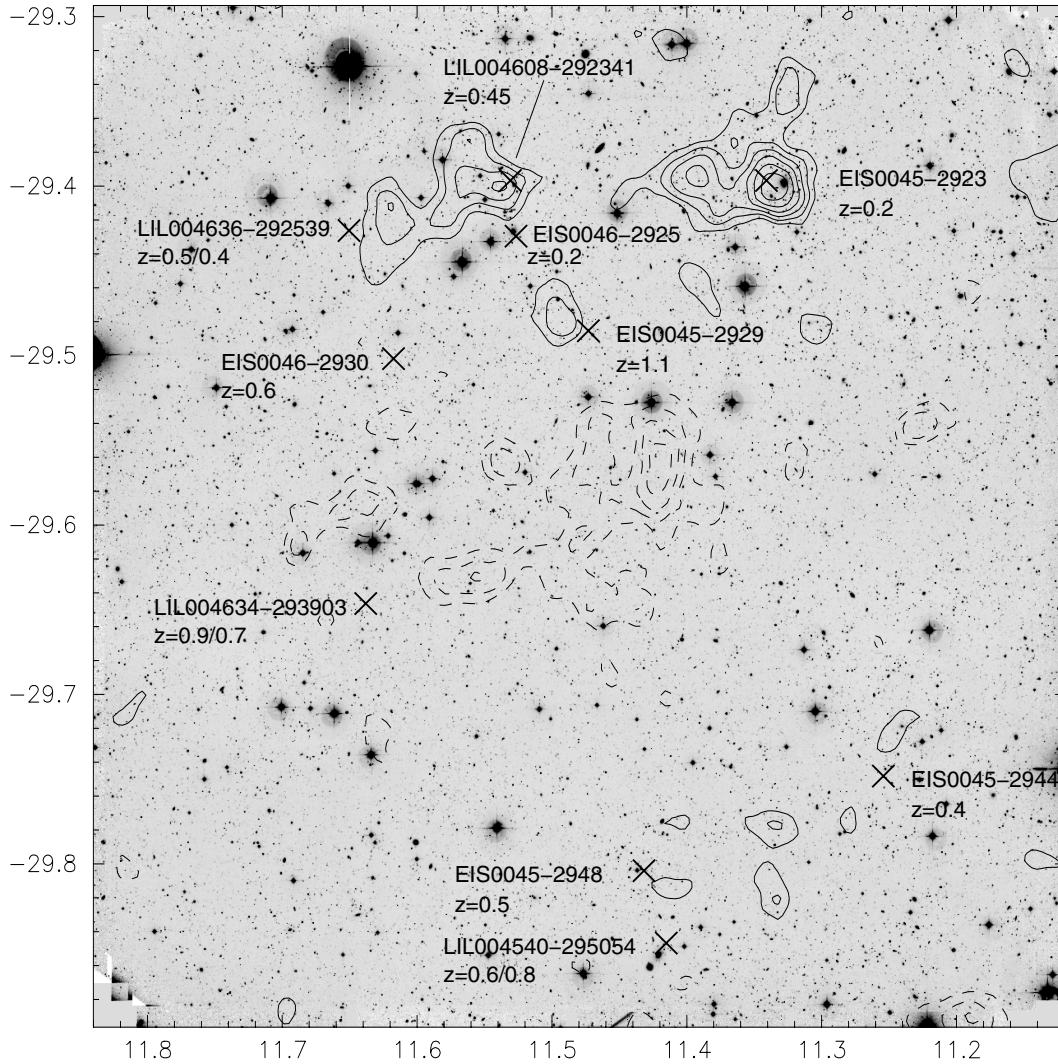


Fig. 4. S -statistics of the full SGP field. The contours start at the 2σ -level and go in steps of 0.5σ . Dashed lines denote negative signals, i.e. underdense regions. The extended depression near the field centre is significant up to the 4σ -level. The colour-selected cluster candidates are indicated by crosses. The axes denote RA and Dec in degrees. North is up and East is left.

References

- Bartelmann, M., & Schneider, P. 2001, *Phys. Rep.*, 340, 291
Dahle, H., Pedersen, K., Lilje, P. B., Maddox, S. J., & Kaiser, N. 2003, *ApJ*, 591, 662
Erben, T., van Waerbeke, L., Mellier, Y., et al. 2000, *A&A*, 355, 23
Erben, T., van Waerbeke, L., Bertin, E., Mellier, Y., & Schneider, P. 2001, *A&A*, 336, 717
Gray, M. E., Taylor, A. N., Meisenheimer, K., et al. 2002, *ApJ*, 568, 141
Kaiser, N. 1995, *ApJ*, 439, L1
Kaiser, N., Squires, G., & Broadhurst, T. 1995, *AJ*, 449, 460
Kruse, G., & Schneider, P. 1999, *MNRAS*, 302, 821
Lobo, C., Iovino, A., Lazzati, D., & Chincarini, G. 2000, *A&A*, 360, 869
Maoli, R., van Waerbeke, L., Mellier, Y., et al. 2001, *A&A*, 368, 766
Miralles, J. M., Erben, T., Hämmerle, H., et al. 2002, *A&A*, 388, 68
Miyazaki, S., Hamana, T., Shimasaku, K., et al. 2002, *ApJ*, 580, 97
Navarro, J., Frenk, C., & White, S. 1996, *ApJ*, 642, 563
Olsen, L. F., Scodreggio, M., da Costa, L., et al. 1999, *A&A*, 345, 363
Postman, M., Lubin, L. M., Gunn, J. E., et al. 1996, *AJ*, 111, 615
Schirmer, M., Erben, T., Schneider, P., et al. 2003, *A&A*, 407, 869
Schneider, P. 1996, *MNRAS*, 283, 837
Schneider, P., van Waerbeke, L., Jain, B., & Kruse, G. 1998, *MNRAS*, 296, 873
Seitz, S., & Schneider, P. 1996, *A&A*, 305, 383
Umetsu, K., & Futamase, T. 2000, *ApJ*, 539, L5
Wittman, D., Tyson, J. A., Margoniner, V. E., et al. 2001, *ApJ*, 557, 89
Wittman, D., Margoniner, V. E., Tyson, J. A., et al. 2003, *ApJ*, 597, 218W
Wolf, C., Meisenheimer, K., Rix, H.-W., et al. 2003, *A&A*, 401, 73